

Three-dimensional instability of a multipolar vortex in a rotating flow

Stéphane Le Dizès^{a)}

*Institut de Recherche sur les Phénomènes Hors Équilibre, 12 Avenue Général Leclerc,
F-13003 Marseille, France*

(Received 7 February 2000; accepted 5 July 2000)

In this paper, the elliptic instability is generalized to account for Coriolis effects and higher order symmetries. We consider, in a frame rotating at the angular frequency Ω , a stationary vortex which is described near its center $r=0$ by the stream function written in polar coordinates $\Psi = -(r^2/2) + p(r^n/n)\cos(n\theta)$, where the integer n is the order of the azimuthal symmetry, and p is a small positive parameter which measures the strength of the nonaxisymmetric field. Based on the Lifschitz and Hameiri [Phys. Fluids A **3**, 2644–2651 (1991)] theory, the local stability analysis of the streamline $\Psi = -1/2$ is performed in the limit of small p . As for the elliptic instability [Bayly, Phys. Rev. Lett. **57**, 2160–2163 (1986)], the instability is shown to be due to a parametric resonance of inertial waves when the inclination angle ξ of their wave vector with respect to the rotation axis takes a particular value given by $\cos \xi = \pm 4/(n(1+\Omega))$. An explicit formula for the maximum growth rate of the inertial wave is obtained for arbitrary ξ , Ω , and n . As an immediate consequence, it is shown that a vortex core of relative vorticity W_r (assumed positive) is locally unstable if $\Omega < -(1+n/4)W_r/2$ or $\Omega > (-1+n/4-p(n-1)/2)W_r/2$. The predictive power of the local theory is demonstrated on several vortex examples by comparing the local stability predictions with global stability results. For both the Kirchhoff vortex and Moore and Saffman vortex, it is shown how global stability results can be derived from the local stability analysis using the dispersion relation of normal (Kelvin) modes. These results are compared to those obtained by global methods and a surprisingly good agreement is demonstrated. The local results are also applied to rotating Stuart vortices and compared to available numerical data. © 2000 American Institute of Physics. [S1070-6631(00)01410-0]

I. INTRODUCTION

The emergence of multipolar vortices in rotating fluids is a well-known feature which has been evidenced both experimentally and numerically (see, for instance, Hopfinger and van Heijst¹ and references therein). These vortical structures are usually formed of a central vortex surrounded by several vortices of opposite sign. They are known to appear spontaneously by a 2D inviscid instability from monopolar vortices which have not a monotonous vorticity profile.

These vortices may be unstable with respect to the axisymmetric centrifugal instability. For axisymmetric vortices in a fixed frame, Rayleigh showed that the nondecreasing behavior of the square of the circulation provides a condition for stability. Analogue criteria have been obtained for non-axisymmetric vortices in a fixed frame² and in a rotating frame.^{3,4} Here, we shall not be concerned with the centrifugal instability. We shall assume that the instability is generated by another mechanism associated with the nonaxisymmetry of the vortex.

That the nonaxisymmetry could be a source of instability was first understood by Pierrehumbert⁵ who studied the short-wavelength stability of an elliptic vortex. Bayly⁶ and Waleffe⁷ gave a complete explanation of the instability mechanism in the context of uniform elliptical flows. They

showed that the inertial waves of the vortex could be parametrically excited by the underlying strain field via the vorticity stretching mechanism.⁸ An early explanation was also given in terms of Kelvin modes resonance by Tsai and Widnall⁹ and Moore and Saffman.¹⁰ The inertial wave description was extended and formalized in a more general framework using Lagrangian methods by Lifschitz and Hameiri.¹¹ This has permitted to consider additional effects such as stratification,¹² rotation,^{13–15} stretching,¹⁶ nonuniformity,^{17–21} and time-dependence.^{22–24}

Vortices with a fold symmetry larger than 2 were considered only recently.^{25–28} Le Dizès and Eloy²⁵ showed that in a fixed frame an instability similar to the “elliptical instability” exists in triangular and quadripolar vortices. This instability was analyzed by global techniques for a Rankine vortex in Eloy and Le Dizès.²⁶ The first experimental evidence was given by Eloy, Le Gal, and Le Dizès.^{27,28} Our goal is here to extend the local analysis of Le Dizès and Eloy²⁵ by considering the additional effects of Coriolis forces.

The paper is organized as follows. In Sec. II the framework of the local stability theory is presented. The general system of equations for the perturbations obtained by Bayly *et al.*²³ is extended to account for Coriolis forces. In Sec. III, these equations are solved in a frame rotating at the angular frequency Ω for the basic flow given by the stream function

^{a)}Electronic mail: ledizes@marius.univ-mrs.fr

$$\Psi = -\frac{r^2}{2} + p \frac{r^n}{n} \cos(n\theta),$$

where the integer n is the order of the azimuthal symmetry, and p is a small positive parameter which measures the strength of the nonaxisymmetric field. The local stability properties of the streamline $\Psi = -1/2$ are obtained by an asymptotic method in the limit of small p . An explicit formula for the leading order maximum growth rate is derived in terms of n , Ω , and the wave vector inclination angle ξ . The consequences of this formula are detailed in Sec. III B. In Sec. IV A, the results are applied to a deformed Rankine vortex. It is shown how global results can be obtained by summing local perturbations to form normal (Kelvin) modes. The results obtained by this approach are compared to available global stability results for the Kirchhoff vortex^{29,30} and the Moore–Saffman vortex.^{10,26,31} In Sec. IV B, the local growth rate formula is applied to Stuart vortices in a rotating frame. For a fixed wave number perturbation, it is shown how the maximum growth rate and the size of the interval of unstable rotation rates can be obtained from the value of the most dangerous rotation rate. The results are compared to numerical data from Leblanc and Cambon²⁰ and Potylitsin and Peltier.³²

II. GEOMETRICAL OPTICS STABILITY EQUATIONS IN A ROTATING FRAME

Let $\mathbf{U}(\mathbf{x})$ be the velocity field of a 2D inviscid steady flow in a frame rotating at the angular frequency Ω . In the geometrical optics stability theory,^{1,23} one considers localized 3D short-wavelength perturbations. At leading order with respect to a characteristic wavelength ϵ , the perturbation velocity is written in the geometrical optics, or WKB form

$$\mathbf{u}(\mathbf{x}, t) = \mathbf{a}(\mathbf{x}, t) \exp\left(\frac{i}{\epsilon} \Phi(\mathbf{x}, t)\right), \tag{1}$$

where the amplitude $\mathbf{a}(\mathbf{x}, t)$ and phase $\Phi(\mathbf{x}, t)$ are real functions dependent on space $\mathbf{x} = (x, y, z)$ and time t . The local (renormalized) wave number is defined from Φ by

$$\mathbf{k} = \nabla \Phi. \tag{2}$$

Substituting Eq. (1) in the linearized Euler equations and equating terms of same order in ϵ lead to a system of equations for \mathbf{a} and \mathbf{k} . As shown by Lifschitz and Hameiri,¹¹ this system reduces to simple ordinary differential equations along the streamlines of the basic flow which are defined by

$$\frac{d\mathbf{X}}{dt} = \mathbf{U}(\mathbf{X}, t). \tag{3}$$

In a frame rotating at the angular frequency Ω , the Lifschitz and Hameiri equations read¹⁵

$$\frac{d\mathbf{k}}{dt} - \mathcal{L}^T(t)\mathbf{k}, \tag{4a}$$

$$\frac{d\mathbf{a}}{dt} = \left[\left(\frac{2\mathbf{k}\mathbf{k}^T}{|\mathbf{k}|^2} - I \right) \mathcal{L}(t) + \left(\frac{\mathbf{k}\mathbf{k}^T}{|\mathbf{k}|^2} - I \right) \mathcal{C} \right] \mathbf{a}, \tag{4b}$$

$$\mathbf{k} \cdot \mathbf{a} = 0, \tag{4c}$$

where d/dt denotes Lagrangian derivatives $d/dt = \partial/\partial t + \mathbf{U} \cdot \nabla$, I the identity matrix, $\mathcal{L}(t) = \nabla \mathbf{U}(\mathbf{X}(t), t)$ and

$$\mathcal{C} = \begin{pmatrix} 0 & -2\Omega & 0 \\ 2\Omega & 0 & 0 \\ 0 & 0 & 0 \end{pmatrix}. \tag{5}$$

Equation (4c) is the condition of incompressibility. That condition is always fulfilled if Eqs. (4a) and (4b) are solved from an initial condition $(\mathbf{X}_0, \mathbf{k}_0, \mathbf{a}_0)$ which satisfies $\mathbf{k}_0 \cdot \mathbf{a}_0 = 0$. Lifschitz and Hameiri proved that if $\mathbf{a}(t)$ grows indefinitely, the nonviscous flow is unstable. This is also true in a viscous flow,^{33,1} if the characteristic wavelength ϵ is larger than $\sqrt{\nu/s}$ where ν is the kinetic viscosity and s the maximum inviscid growth rate of \mathbf{a} . On a closed streamline, stability is naturally analyzed by looking at the behavior of \mathbf{a} after one revolution. The initial position on the streamline is not important as it does not modify the growing character of \mathbf{a} . For this reason, a single initial position by streamline is in general taken. Note also that Eq. (4a) for \mathbf{k} is decoupled and Eq. (4b) does not depend on $|\mathbf{k}|$ so one can choose without restriction $|\mathbf{k}_0| = |\mathbf{a}_0| = 1$.

Equations (3) and (4a) also imply that $\mathbf{k} \cdot \mathbf{U}$ is conserved along the streamlines. In order to avoid the stretching of the wave vector, Sipp and Jacquin²¹ showed that \mathbf{k} and \mathbf{U} must remain orthogonal, i.e., $\mathbf{k} \cdot \mathbf{U} = 0$. Otherwise, $|\mathbf{k}|$ increases at each revolution and the perturbation is damped by viscous effects at large time.³³ Finally, if one assumes $\mathbf{k}_0 \cdot \mathbf{U}(\mathbf{X}_0) = 0$, the initial wave vector \mathbf{k}_0 only depends on the angle ξ of the wave vector with respect to the rotation axis of the frame.

In a fixed frame $\Omega = 0$, Bayly, Holm, and Lifschitz²³ showed that Eq. (4b) can be reduced to a system of two equations for

$$\mathbf{V} = \begin{pmatrix} \frac{|\mathbf{k}|}{|\mathbf{k}_\perp|} (\mathbf{k}_\perp \cdot \mathbf{a}_\perp) \\ \frac{|\mathbf{k}|}{|\mathbf{k}_\perp|} (\mathbf{k}_\perp \wedge \mathbf{a}_\perp) \end{pmatrix}, \tag{6}$$

where \perp denotes the projection in the plane perpendicular to the rotation axis. Below the index z will denote the component along the rotation axis. A similar reduction can be carried out in a rotating frame. It yields the system

$$\frac{d\mathbf{V}}{dt} = \mathcal{N} \mathbf{V}, \tag{7}$$

with

$$\mathcal{N} = \begin{pmatrix} -\frac{k_z^2 (\mathcal{L}_\perp \mathbf{k}_\perp \cdot \mathbf{k}_\perp)}{|\mathbf{k}|^2 |\mathbf{k}_\perp|^2} & \frac{2k_z^2 (\mathcal{L}_\perp \mathcal{J} \mathbf{k}_\perp \cdot \mathbf{a}_\perp)}{|\mathbf{k}|^2 |\mathbf{k}_\perp|^2} + 2\Omega \frac{k_z^2}{|\mathbf{k}|^2} \\ -2\Omega - W_z & \frac{k_z^2 (\mathcal{L}_\perp \mathbf{k}_\perp \cdot \mathbf{a}_\perp)}{|\mathbf{k}|^2 |\mathbf{k}_\perp|^2} \end{pmatrix}, \tag{8}$$

where W_z is the (relative) vorticity of the basic flow in the rotating frame and

$$\mathcal{J} = \begin{pmatrix} 0 & 1 \\ -1 & 0 \end{pmatrix}.$$

The goal of this paper is to resolve Eqs. (3), (4a), and (7) for a family of 2D solutions which generically describe the flow in the core of a nonaxisymmetric vortex.

III. LOCAL STABILITY ANALYSIS OF A VORTEX CORE

In a frame rotating at the rotation rate Ω , consider the 2D basic flow described by the stream function (in polar coordinates)

$$\Psi(r, \theta; p) = -\frac{r^2}{2} + p \frac{r^n}{n} \cos(n\theta), \tag{9}$$

where n is an integer larger than 1 and p a real positive parameter. This flow is the superposition of a rotational field of uniform vorticity (first term) and of a multipolar irrotational strain field (second term) characterized by its fold-symmetrical order n and its strength p . As explained by Le Dizès and Eloy,²⁵ it describes the core of a 2D nonviscous vortex in equilibrium with an external strain field which exhibits an n -fold symmetry. For $n=2$ and $n=3$, Eq. (9) is the generic expression for the stream function of a stationary vortex (in a rotating frame) near its center as it corresponds to the first terms of its Taylor expansion with respect to the distance to the vortex axis. This is also the case for larger n if one assumes that the vorticity is sufficiently uniform in the vortex core. In particular, for all n , Eq. (9) is the stream function of a Rankine vortex deformed by either a weak external rotating n -fold symmetrical strain field or a small 2D Kelvin mode of azimuthal wave number n . Accordingly, Ω is either the rotation rate of the external field or the angular frequency of the Kelvin mode. These two cases correspond to generalized Moore–Saffman vortices and generalized Kirchoff vortices which will be analyzed in detail in Sec. IV A. In the following, we focus on local perturbations which grow within the basic flow described by Eq. (9). The external strain field generated by boundaries or distant vortices is not considered in the analysis.

A. Perturbation analysis

In Le Dizès and Eloy,²⁵ the local stability of Eq. (9) was studied without the small p restriction but in a fixed frame ($\Omega=0$). Here, we focus on the additional effects of rotation but limit the analysis to small p . Our main objective is to obtain an explicit formula for the leading order growth rate in the limit of small p that involves n and Ω .

For this purpose, we carry out an asymptotic analysis with respect to $p \rightarrow 0$. Following the classical procedure of perturbation analysis,³⁴ all the quantities are expanded in power of p :

$$\Omega = \Omega_0 + p\Omega_1 + \dots, \tag{10a}$$

$$\mathbf{X} = \mathbf{X}_0 + p\mathbf{X}_1 + \dots, \tag{10b}$$

$$\mathbf{k} = \mathbf{k}_0 + p\mathbf{k}_1 + \dots, \tag{10c}$$

$$\mathbf{V} = \mathbf{V}_0 + p\mathbf{V}_1 + \dots, \tag{10d}$$

$$\mathcal{L} = \mathcal{L}_0 + p\mathcal{L}_1 + \dots, \tag{10e}$$

$$\mathcal{N} = \mathcal{N}_0 + p\mathcal{N}_1 + \dots. \tag{10f}$$

At leading order, the basic flow is a solid body rotation. The solution of Eq. (3) is then just $\mathbf{X}_{0\perp} = [\cos(t + \theta_0), \sin(t + \theta_0)]$ where θ_0 is the initial azimuthal angle. The equation for \mathbf{k}_0 reduces to

$$\frac{d\mathbf{k}_0}{dt} = -\mathcal{L}_0^T \mathbf{k}_0 \quad \text{with} \quad \mathcal{L}_0 = \begin{pmatrix} 0 & -1 & 0 \\ 1 & 0 & 0 \\ 0 & 0 & 0 \end{pmatrix}. \tag{11}$$

This gives with the conditions $\mathbf{k}_0(0) \cdot \mathbf{U}_0(0) = 0$ and $|\mathbf{k}_0(0)| = 1$

$$\mathbf{k}_0 = [\sin \xi_0 \cos(t + \theta_0), \sin \xi_0 \sin(t + \theta_0), \cos \xi_0], \tag{12}$$

where ξ_0 is the angle between the wave vector \mathbf{k}_0 and the rotation axis. Due to the symmetries of Eq. (8) which is invariant by the change \mathbf{k} in $-\mathbf{k}$ and k_z in $-k_z$, we can assume without restriction that $0 \leq \xi_0 < \pi/2$.

Substituting expression (12) in the leading order equation for \mathbf{V}_0 leads to

$$\frac{d\mathbf{V}_0}{dt} = \begin{pmatrix} 0 & 2(\Omega_0 + 1)\cos^2 \xi_0 \\ -2(\Omega_0 + 1) & 0 \end{pmatrix} \mathbf{V}_0. \tag{13}$$

The general solution of that equation is

$$\mathbf{V}_0 = A_a \mathbf{V}_a(t) + A_b \mathbf{V}_b(t), \tag{14}$$

where A_a and A_b are two real constants and

$$\begin{aligned} \mathbf{V}_a &= [\cos \xi_0 \sin(\omega(t + \theta_0)), \cos(\omega(t + \theta_0))], \\ \mathbf{V}_b &= [\cos \xi_0 \cos(\omega(t + \theta_0)), +\sin(\omega(t + \theta_0))], \end{aligned} \tag{15}$$

with

$$\omega = 2(\Omega_0 + 1)\cos \xi_0. \tag{16}$$

The solution $\mathbf{V}_0 \exp(i\mathbf{k}_0(t) \cdot \mathbf{x})$ is the well-known *inertial* wave solution of solid body rotating flows.³⁵ Its wave vector rotates periodically with respect to the k_z -axis with the same frequency as the basic flow and with a constant inclination angle ξ_0 ; its amplitude is periodic with a frequency $\omega = W_a \cos \xi_0$, where W_a is the absolute vorticity of the flow.

At the next order, the trajectory is slightly deformed: the streamline $\Psi = -1/2$ is given by

$$r = 1 + \frac{p}{n} \cos(n\theta) + O(p^2), \tag{17a}$$

$$\frac{d\theta}{dt} = 1 - p \cos(n\theta) + O(p^2), \tag{17b}$$

and the correction of the velocity tensor reads

$$\mathcal{L}_{1\perp} = (n-1) \begin{pmatrix} \sin[(n-2)\theta] & \cos[(n-2)\theta] \\ \cos[(n-2)\theta] & -\sin[(n-2)\theta] \end{pmatrix}. \tag{18}$$

This permits to write the equation for \mathbf{k}_1 as follows:

$$\frac{d\mathbf{k}_1}{d\theta} = -\mathcal{L}_{0\perp} \mathbf{k}_1 - (\mathcal{L}_{1\perp} + \cos(n\theta)\mathcal{L}_{0\perp}) \mathbf{k}_0, \tag{19}$$

which yields

$$\mathbf{k}_1 = \frac{\sin \xi_0}{2n} \begin{pmatrix} (1-2n)\cos[(n-1)\theta] + \cos[(n+1)\theta] \\ (1-2n)\sin[(n-1)\theta] + \sin[(n+1)\theta] \\ 0 \end{pmatrix},$$

$$+ \xi_1 \begin{pmatrix} \cos \xi_0 \cos \theta \\ \cos \xi_0 \sin \theta \\ -\sin \xi_0 \end{pmatrix}, \tag{20}$$

where $\theta(t)$ is obtained from Eq. (17b) and the condition $\theta(0) = \theta_0$. The second term is an homogeneous solution \mathbf{k}_{1h} which is such that the wave vector $\mathbf{k}_0 + p\mathbf{k}_{1h}$ of the inertial wave satisfies $|\mathbf{k}_0 + p\mathbf{k}_{1h}| = 1 + O(p^2)$ and $(\mathbf{k}_0 + p\mathbf{k}_{1h}) \cdot \mathbf{e}_z = \cos(\xi_0 + p\xi_1) + O(p^2)$. Note that if one had considered \mathbf{k}_0

such that $\mathbf{k}_0 \cdot \mathbf{U}_0 \neq 0$, the inhomogeneous solution would contain terms proportional to θ ; this would characterize a degeneracy which would in the present case signify that the wave vector amplitude should increase at each revolution with an angular growth rate proportional to p . This situation has been excluded because it always leads to large wave vectors damped by viscosity.

The equation for \mathbf{V}_1 can be written as

$$\frac{d\mathbf{V}_1}{d\theta} = \mathcal{N}_0 \mathbf{V}_1 + \mathcal{N}_1 \mathbf{V}_0, \tag{21}$$

where \mathcal{N}_0 is the operator in Eq. (13) and

$$\mathcal{N}_1 = \begin{pmatrix} (n-1)\cos^2 \xi_0 \sin(n\theta) & \alpha \cos(n\theta) + 2\Omega_1 \cos^2 \xi_0 - 4(1 + \Omega_0)\xi_1 \sin \xi_0 \cos \xi_0 \\ -2(\Omega_0 + 1)\cos(n\theta) - 2\Omega_1 & -(n-1)\cos^2 \xi_0 \sin(n\theta) \end{pmatrix}, \tag{22}$$

with

$$\alpha = 2(n + \Omega_0)\cos^2 \xi_0 + 4(n - 1/n)(1 + \Omega_0)\sin^2 \xi_0. \tag{23}$$

The form of Eqs. (15) and (22) guarantees that the forcing term $\mathcal{N}_1 \mathbf{V}_0$ is a sum of terms oscillating at the frequencies $|\omega|$ and $|n \pm \omega|$. The terms oscillating at $|\omega|$ are proportional to ξ_1 or Ω_1 . They are always resonant with the homogeneous solutions of Eq. (21). This degeneracy induces an $O(p)$ frequency correction of the inertial wave but it does not create any instability. By contrast, when the terms oscillating at the frequency $|n \pm \omega|$ resonate with the homogeneous solutions of Eq. (21), i.e., when their frequency matches the inertial wave frequency, the degeneracy in general yields an instability. There are two conditions of self-resonance which are $\omega = n - \omega$ and $\omega = -n - \omega$. They give

$$4(\Omega_0 + 1)\cos \xi_0 = \epsilon_0 n, \tag{24}$$

where $\epsilon_0 = \pm 1$. The instability growth rate associated with each resonance is calculated using the classical procedure of multiple scales analysis.³⁴ An additional dependence on the slow angular scale $\Theta = p\theta$ is introduced in the amplitudes A_a and A_b of the inertial wave in such a way that the degeneracy is suppressed. Here, a weak exponential growth is expected so A_a and A_b can be searched in the form

$$A_a = e^{\sigma_1 \Theta} A_a^{(0)}, \quad A_b = e^{\sigma_1 \Theta} A_b^{(0)}, \tag{25}$$

where $A_a^{(0)}$ and $A_b^{(0)}$ are real constants and σ_1 the angular growth rate. The slow-angular variation of \mathbf{V}_0 modifies Eq. (21) which now contains an additional term $-\sigma_1 \mathbf{V}_0$ on the right-hand side. As explained in text books,³⁴ this additional term permits to suppress the degeneracy by enforcing the orthogonality of the forcing terms with respect to the adjoint modes of the homogeneous equation. For the scalar product $\langle f/g \rangle = \int_0^{2\pi} f g^* d\theta$, the adjoint modes are

$$\mathbf{V}_a^\perp = [\epsilon_0 \sin(n\theta/2), \cos \xi_0 \cos(n\theta/2)], \tag{26a}$$

$$\mathbf{V}_b^\perp = [\cos(n\theta/2), -\epsilon_0 \cos \xi_0 \sin(n\theta/2)]. \tag{26b}$$

Thus the orthogonality conditions leads to two linear homogeneous equations for the constants $A_a^{(0)}$ and $A_b^{(0)}$ which depend on the parameter σ_1 . The condition of solvability of this system finally gives

$$\sigma_1^2 = \frac{\langle \mathcal{N}_1 \mathbf{V}_b | \mathbf{V}_a^\perp \rangle \langle \mathcal{N}_1 \mathbf{V}_a | \mathbf{V}_b^\perp \rangle}{\langle \mathbf{V}_a | \mathbf{V}_a^\perp \rangle \langle \mathbf{V}_b | \mathbf{V}_b^\perp \rangle}, \tag{27}$$

which surprisingly reduces to a simple expression:

$$\sigma_1 = \frac{\sqrt{(n-1)^2(n+4(1+\Omega_0))^4 - K^2}}{64(1+\Omega_0)^2}, \tag{28}$$

with

$$K = 32(1 + \Omega_0)(n\Omega_1 - (1 + \Omega_0)[16(1 + \Omega_0)^2 - n^2]^{1/2}\xi_1). \tag{29}$$

As, at leading order, $\theta = t + \theta_0$ along the streamline trajectories, σ_1 also corresponds to a temporal growth rate. Thus the temporal growth rate in terms of the initial variables (nondimensionalized by the half of the relative vorticity) is

$$\sigma = \sigma_1 p + O(p^2). \tag{30}$$

This expression applies only if the condition of resonance Eq. (24) is satisfied, or equivalently if the leading order wave vector angle ξ_0 of the inertial wave satisfies

$$\cos \xi_0 = \mathbf{k}_0 \cdot \mathbf{e}_z = \frac{\epsilon_0 n}{4(1 + \Omega_0)}. \tag{31}$$

In order to plot σ , it is necessary to transcribe expressions (28)–(31) in terms of the initial variables ξ and Ω . For instance, this can be done by fixing $\xi = \xi_0$ and by replacing Ω_0 by its expression in terms of ξ . This leads to

$$\sigma = \frac{1}{4} \sqrt{(n-1)^2(1 + \epsilon_0 \cos \xi)^4 p^2 - 4(n - 4\epsilon_0(1 + \Omega)\cos \xi)^2}, \tag{32}$$

which is equivalent to Eqs. (28)–(30) with condition (31) if one expands $\Omega = \Omega_0 + p\Omega_1$ and $\xi = \xi_0 + p\xi_1$.

In the above formula, Ω corresponds to $1/\text{Ro}$ where the Rossby number Ro is the ratio of the relative vorticity in the

vortex center by twice the angular frequency of the rotating frame. Here the relative vorticity is $W_r=2$ and the absolute vorticity is $W_a=2(1+\Omega)=2(1+1/Ro)$.

B. Local stability properties

Expression (32) shows that for a fixed ξ , there is instability as soon as Ω satisfies

$$\left| \Omega - \frac{n}{4 \cos \xi} + 1 \right| < \frac{(n-1)(1+\cos \xi)^2}{8|\cos \xi|} p, \tag{33}$$

or

$$\left| \Omega + \frac{n}{4 \cos \xi} + 1 \right| < \frac{(n-1)(1-\cos \xi)^2}{8|\cos \xi|} p. \tag{34}$$

Inversely, for a fixed Ω , one can similarly show that the unstable wave vector angles ξ are given by

$$\left| \cos \xi - \frac{n}{4(1+\Omega)} \right| < \frac{(n-1)(n+4(1+\Omega))^2}{128|1+\Omega|^3} p, \tag{35}$$

and

$$\left| \cos \xi + \frac{n}{4(1+\Omega)} \right| < \frac{(n-1)(n+4(1+\Omega))^2}{128|1+\Omega|^3} p. \tag{36}$$

Conditions (35) and (36) were also given by Bayly *et al.*²³ for $n=2$. For a fixed angle ξ , there are two local maximum growth rates $\sigma_{\max}^{\pm}(\xi)$ associated with each resonance, i.e., $\epsilon_0 = \pm 1$. In each case, the maximum growth rate $\sigma_{\max}^{\pm}(\xi)$ over all the possible rotation rates Ω is obtained when the resonance is perfect, that is for

$$\Omega_{\max}^+(\xi) = -1 + \frac{n}{4 \cos \xi}, \tag{37}$$

or

$$\Omega_{\max}^-(\xi) = -1 - \frac{n}{4 \cos \xi}. \tag{38}$$

Expressions for $\sigma_{\max}^+(\xi)$ and $\sigma_{\max}^-(\xi)$ obtained from Eq. (32) are particularly simple. They read

$$\sigma_{\max}^+(\xi) = (\cos(\xi/2))^4 s, \tag{39}$$

and

$$\sigma_{\max}^-(\xi) = (\sin(\xi/2))^4 s, \tag{40}$$

where s is the local strain rate on the streamline

$$s = (n-1)p. \tag{41}$$

The graphs of $\Omega_{\max}^{\pm}(\xi)$ and $\sigma_{\max}^{\pm}(\xi)/s$ are displayed for $0 \leq \xi < \pi/2$ in Fig. 1. From Fig. 1(a), one clearly sees that the resonance associated with $\epsilon_0=1$ is more dangerous than the other one $\epsilon_0=-1$ (except at $\xi=\pi/2$). The largest maximum growth rate is therefore $\sigma_{\max}^+(\xi)$ for $0 \leq \xi < \pi/2$. Expression (39) also shows that the largest maximum growth rate is always smaller or equal than the local strain rate. This is in agreement with the interpretation of the instability by the vortex stretching mechanism (see Orszag and Patera,⁸ Waleffe,⁷ Huerre and Rossi,³⁶ Eloy and Le Dizès²⁶). Moreover, one can check that there is a direct correlation between

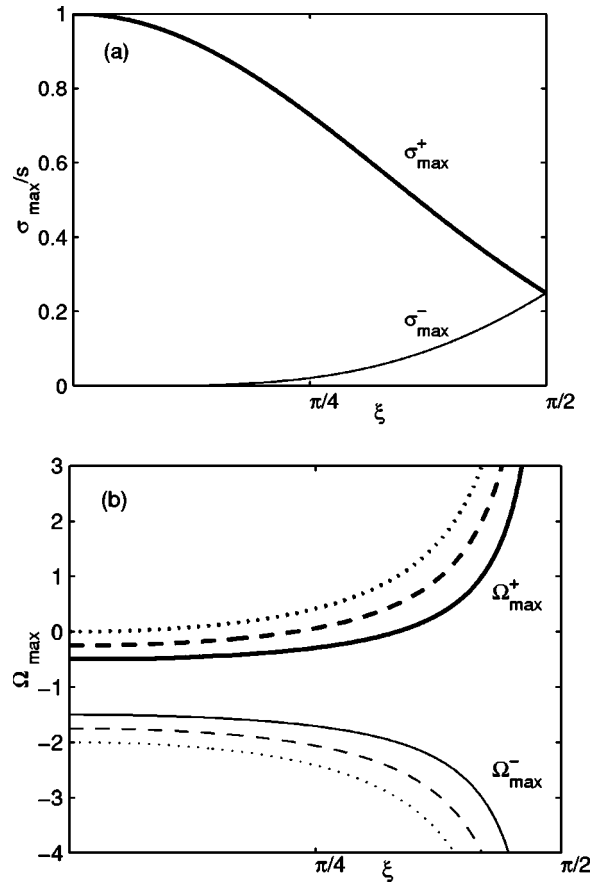


FIG. 1. Normalized maximum growth rate σ_{\max}^{\pm}/s (a) and most dangerous rotation rate Ω_{\max}^{\pm} (b) as a function of ξ . In (b), solid line: $n=2$, dashed line: $n=3$, dotted line: $n=4$. On both figures, the thick lines correspond to the most unstable resonance ($\epsilon_0=1$).

the good alignment of the perturbation vorticity with the direction of stretching and the largeness of the growth rate. In particular, for the resonant vertical wave vectors ($\xi=0$), vorticity is oriented along a direction which makes an angle $-\epsilon_0 n \theta/2$ with respect to the radial polar vector $e_r(\theta)$ for all θ . For $\epsilon_0=1$, this direction is exactly the same as the direction of stretching everywhere along the streamline. The alignment of vorticity with the stretching direction is therefore maximized in that case, which justifies both the maximization of the instability and the equality of the growth rate with the local strain rate.²⁶ Inversely, for the other resonance $\epsilon_0=-1$, the angle between the vorticity direction and the direction of stretching is equal to $n\theta$ at the azimuthal position θ on the streamline. This implies that, during a revolution on the streamline, vorticity is as much compressed as stretched. Based on the vortex stretching mechanism, it is therefore again not surprising that the growth rate cancels in that case. For a fixed Ω , the maximum growth rate $\sigma^{\max}(\Omega)$ over all the possible angles ξ can also be obtained from Eq. (32). However, contrary to σ_{\max} , its value depends on both n and p . Formula (32) leads to the following results.

- For $\Omega \leq -1 - n/4$ and $\Omega \geq -1 + n/4$, $\sigma^{\max}(\Omega)$ is up to $O(p^2)$ terms given by expression (39), where $\epsilon_0 \cos \xi$ is replaced by $n/4/(1+\Omega)$, i.e.,

$$\sigma^{\max}(\Omega) = \frac{(n+4(1+\Omega))^2}{64(1+\Omega)^2} (n-1)p + O(p^2). \quad (42)$$

In this interval of Ω , the most dangerous angle $\xi^{\max}(\Omega)$ in $(0, \pi/2)$ is given by

$$\cos[\xi^{\max}(\Omega)] = \frac{n}{4|1+\Omega|} + O(p^2). \quad (43)$$

Note that there is a single resonance with $0 \leq \xi \leq \pi/2$. One therefore must take $\epsilon_0 = 1$ for $\Omega \geq -1 + n/4$ but $\epsilon = -1$ for $\Omega \leq -1 - n/4$. The other resonance which corresponds to a value of ξ in $(\pi/2, \pi)$ is obtained by the transformation $\xi^{\max} \rightarrow \pi - \xi^{\max}$. Due to the symmetry mentioned above, this second resonance shares exactly the same properties as the first one and does not have to be considered.

- For $-1 + n/4 - p(n-1)/2 < \Omega < -1 + n/4$, the resonance is imperfect. One has $\xi^{\max}(\Omega) = 0$ and

$$\sigma^{\max}(\Omega) = \sqrt{(n-1)^2 p^2 - 4(\Omega + 1 - n/4)^2} + O(p^2). \quad (44)$$

- For $-1 - n/4 < \Omega < -1 + n/4 - p(n-1)/2$, there is no resonance. Up to $O(p^2)$ terms, the flow is then locally stable.

For $n=2$, expression (42) was first given by Miyazaki *et al.*³⁰

The dependence of the stability properties on n and p is illustrated in Figs. 2 and 3, respectively. In Fig. 3(a), $\sigma^{\max}(\Omega)$ is plotted near $\Omega = -1 + n/4$ for $n=2$ and two positive values of p . The corresponding most dangerous angle ξ^{\max} is plotted in Fig. 3(b). It is interesting to note that the interval of Ω where purely axial inertial waves ($\xi=0$) are the most unstable grows with p . In addition, it is clearly seen that the region of instability enlarges and the growth rate increases as p grows. This can also be observed in Fig. 4 where are shown contour plots of σ/s in the (Ω, ξ) plane for several values of p and n .

For small p and whatever n , the interval without resonance contains the value $\Omega = -1$ for which the absolute vorticity of the vortex vanishes. It immediately follows that the core of a multipolar vortex of zero absolute vorticity is 3D stable. This is in agreement with the results obtained for uniform elliptic vortices.^{13,14} Note also that, for small p , the interval without resonance contains negative values of Ω only if $n=2,3,4$. This means that all the cyclonic vortices with a fold-symmetry of order smaller than 5 are locally unstable. For larger value of n , the rotation rate must be superior to $(n-4-2p(n-1))/4$ to destabilize the vortex. It is worth mentioning that the instability is not suppressed by strong rotation. For both strong cyclonic and strong anticyclonic rotations, the stability properties become identical: the maximum growth rate $\sigma^{\max}(\Omega)$ tends to $s/4$ and $\xi^{\max}(\Omega)$ goes to $\pi/2$ as $\Omega \rightarrow \pm \infty$. The main effect of strong rotation is then to force the instability to become two-dimensional. This is reminiscent of the Taylor–Proudman theorem.³⁵ Note also that if the growth rate was normalized with the absolute vorticity, the vorticity would disappear in the limit $|\Omega| \rightarrow +\infty$ in agreement with the 2D stability of the flow.

The asymptotic results obtained here are in agreement with recent computations by Sipp *et al.*³⁷ They computed the

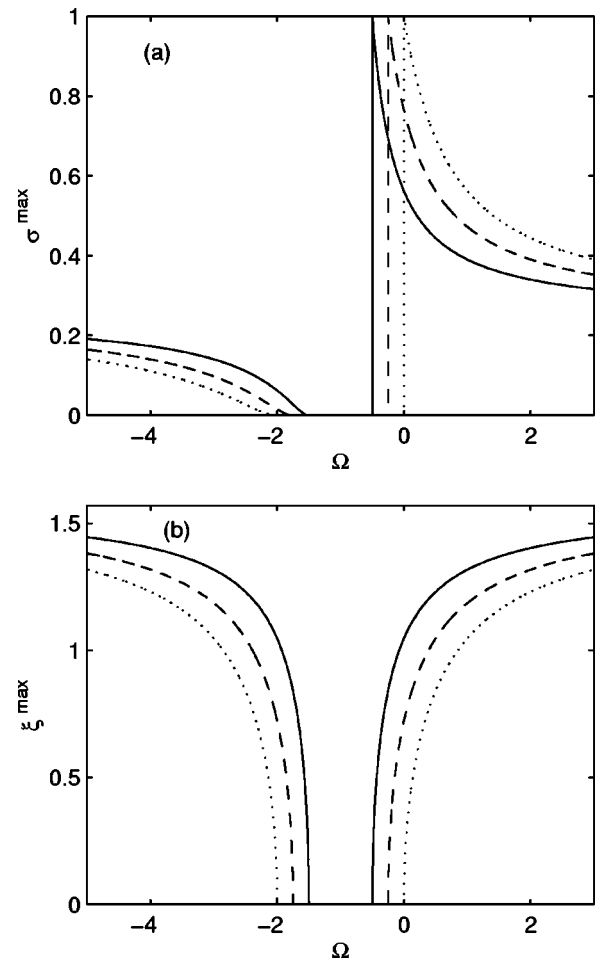


FIG. 2. Normalized maximum growth rate σ^{\max}/s (a) and wave vector angle ξ^{\max} (b) versus Ω in the limit $p \rightarrow 0$ for various n . Solid line: $n=2$; dashed line: $n=3$; dotted line: $n=4$.

local stability properties of a Taylor–Green vortex of aspect ratio 2. Although $p=0.6$ in their case, their results compared surprisingly well with our small p analysis. In particular, they obtained, as we did for $n=2$, that the local growth rate is maximum and proportional to the local strain rate (which is 0.3 in their case) for $\Omega = -1/2$ and axial wave vectors ($\xi=0$). They showed that axial wave vectors were the most unstable for $-0.8 < \Omega < -0.33$ which is very close to what we have obtained (see Fig. 3). They also obtained a stabilization of the elliptical instability for anticyclonic rotation between approximately -1.33 and -0.8 which favorably compares with our stabilization interval: $-1.5 < \Omega < -0.8$. For strong cyclonic and anticyclonic rotation, they observed that the growth rate tends to the quarter the local strain rate and that the perturbations becomes two-dimensional as predicted here. Sipp *et al.*³⁷ also performed a global stability analysis and obtained the form of the eigenmodes associated with the elliptical instability. They confirmed the relevance of the local stability results by showing that the most unstable eigenmode is localized in the vortex core and that its growth rate is close to the local growth rate of the elliptic center with an accuracy increasing with the wave number. Other examples given in the next section will also demonstrate the predictive power of the local stability results.

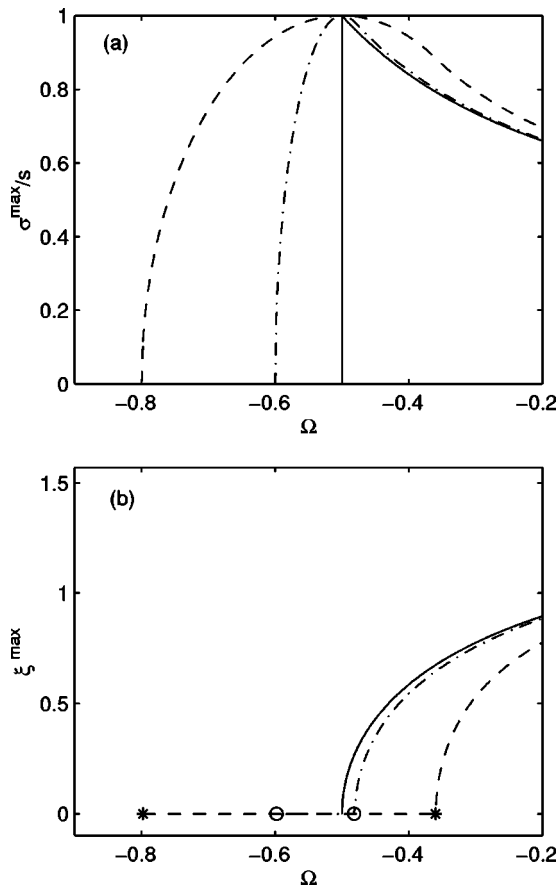


FIG. 3. Normalized maximum growth rate σ^{\max}/s (a) and wave vector angle ξ^{\max} versus Ω for $n=2$ and various p . Solid line: $p \rightarrow 0$; Dash-dotted line: $p=0.2$; Dotted line: $p=0.6$. The symbols \circ and $*$ indicate the interval in which axial wave vectors are the most unstable for $p=0.2$ and $p=0.6$, respectively.

To close this section on local stability results, it is worth mentioning that viscous effects on the perturbations can be easily taken into account^{38,33} by adding in expression (32) the viscous damping rate

$$\sigma_v = -\nu |\mathbf{k}/\varepsilon|^2, \tag{45}$$

where ν is the kinematic viscosity. This damping rate favors the largest wave numbers and introduces a cutoff wave number proportional to $\sqrt{s/\nu}$ above which the instability disappears.

IV. APPLICATIONS TO VORTEX EXAMPLES

A. Moore–Saffman vortex, Kirchhoff vortex, and higher order generalizations

Rankine vortex is a circular region of uniform vorticity surrounded by an irrotational flow. Nonaxisymmetric extensions of this nonviscous solution have been considered in numerous works. Kirchhoff (see Saffman³⁹) first considered the case of an elliptic region of uniform vorticity in strain-free environment. His solution was numerically extended by Deem and Zabusky⁴⁰ to vortices with a fold-symmetry of higher order. Moore and Saffman⁴¹ analyzed the nonaxisymmetric deformation generated by a stationary external strain. They obtained an exact solution in closed form for $O(1)$

deformation. Kida⁴² extended both the Moore and Saffman and Kirchhoff solutions by considering an elliptical vortex patch in a uniform rotating strain field.

In this section, we analyze the stability of Moore–Saffman vortex and Kirchhoff vortex and their higher order symmetrical analogues in the limit of small nonaxisymmetric deformations.

When the azimuthal deformation is small, Kirchhoff vortex and its higher order symmetrical extension are at leading order nothing but the Rankine vortex deformed by a 2D linear Kelvin mode of azimuthal wave number 2 or larger (see, for instance, Saffman³⁹). In particular, if p is the amplitude of the Kelvin mode, the deformed Rankine vortex has a stream function of the form³⁹

$$\Psi = -\mu \frac{r^2}{2} + p \frac{r^n}{n} \cos[n(\theta - \omega_n t)], \tag{46}$$

where the angular frequency of the Kelvin mode is $\omega_n = \mu(1 - 1/n)$. This solution is stationary in the frame rotating at the angular frequency $\Omega = \omega_n$. In this rotating frame the stream function is then exactly given by Eq. (9) provided that $\mu = n$, which gives $\Omega = n - 1$.

Similarly, a Rankine vortex subject to a weak stationary multipolar strain field has a stream function in its core given by Eq. (9) with $\Omega = 0$. The case $n=2$ corresponds to the expression for Moore–Saffman vortex in the limit of weak strain.

Using the results of the previous section, the local stability properties of both types of vortices are immediately obtained.

- For the generalized Kirchhoff vortex: Both the most dangerous wave vector angle ξ^{\max} and the maximum growth rate σ^{\max} are independent of the azimuthal symmetry of the vortex. They are given by

$$\cos \xi^{\max} = \frac{1}{4} \tag{47}$$

and

$$\sigma^{\max} = \left(\frac{5}{8}\right)^2 (n-1)p = \left(\frac{5}{8}\right)^2 s, \tag{48}$$

where s is the local strain rate on the streamline. Whatever n , the generalized Kirchhoff vortex is therefore unstable with respect to 3D short-wavelength perturbations and the most unstable local perturbation is independent of n .

- For the generalized Moore–Saffman vortex: The generalized Moore–Saffman vortex is unstable only if $n \leq 4$. The most dangerous wave vector angle ξ^{\max} satisfies

$$\cos \xi^{\max} = \frac{n}{4}, \tag{49}$$

and the maximum growth rate is

$$\sigma^{\max} = \frac{(n+4)^2}{64} (n-1)p = \frac{(n+4)^2}{64} s. \tag{50}$$

These local results provide the maximum possible growth rate but they are unable to predict the stability of the vortex for a given axial wave number nor the spatial structure of the unstable modes. For this purpose it is necessary to

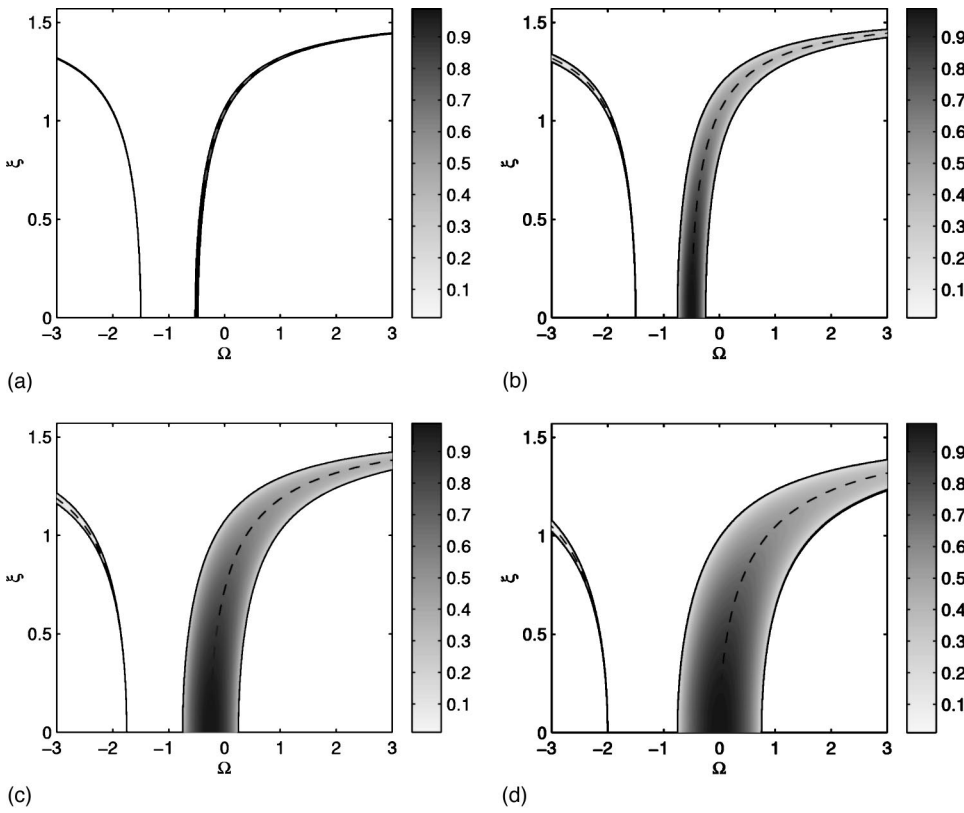


FIG. 4. Contour plot of the growth rate σ/s in the plane (Ω, ξ) where Ω is the rotation rate and ξ the wave vector angle with respect to the rotation axis. The solid line is the limit of the domain of instability [obtained from expression (33)]. The dashed lines are expressions (37) and (38). (a) $n=2, p=0.05$; (b) $n=2, p=0.5$; (c) $n=3, p=0.5$; (d) $n=4, p=0.5$.

build a global perturbation from the unstable inertial waves. This was done by Waleffe⁷ for the elliptic instability in a fixed frame. Here, we slightly extend his analysis to account for the angular rotation of the frame and higher order azimuthal symmetries.

Let us consider the axial velocity v_z of the most unstable inertial waves. This field is, at leading order, proportional to the first component of \mathbf{V} . Using expressions (14)–(16) and equality (24), it reads in cylindrical coordinates (r, θ, z)

$$v_z = A(\theta_0) \cos(n(t + \theta_0)/2 - \phi) e^{ik_r r \cos(\theta - \theta_0 - t)} e^{ik_z z} e^{\sigma t}, \tag{51}$$

where $A(\theta_0)$ is an arbitrary amplitude and

$$k_r = \frac{\sin \xi}{\epsilon},$$

$$k_z = \frac{\cos \xi}{\epsilon},$$

$$\sigma = \frac{1}{4} \sqrt{(1 + \epsilon_0 \cos \xi)^4 s^2 - 4(n-4)|1 + \Omega \cos \xi|^2}, \tag{52}$$

$$\tan \phi = \sqrt{\frac{(1 + \epsilon_0 \cos \xi)^2 s - 2(n-4)|1 + \Omega \cos \xi|}{(1 + \epsilon_0 \cos \xi)^2 s + 2(n-4)|1 + \Omega \cos \xi|}}.$$

Here, in addition, it is implicitly assumed that ξ is close to the most resonant angle ξ_0 in the interval $(0, \pi/2)$ which satisfies Eq. (24) and that $\epsilon_0(1 + \Omega) > 0$. Expression (51) can be used on any streamline of the vortex core (defined by $-1/2 \ll \Psi \ll 0$) provided that one writes the local strain rate as $s = (n-1)r^{n-2}p$.

If one takes $A(\theta_0) = 2e^{im\theta_0}$ and sums expression (51) over the interval $(0, 2\pi)$, we get, in the fixed frame, the following expression for v_z (see Waleffe⁷):

$$v_z = [J_{n/2-m}(k_r r) e^{i(n/2-m)\theta - i\phi} e^{i(m-(n/2-m)\Omega)t} e^{ik_z z} + J_{-(n/2+m)}(k_r r) e^{-i(n/2+m)\theta + i\phi} \times e^{i(m+(n/2+m)\Omega)t} e^{ik_z z}] e^{\sigma t}, \tag{53}$$

where J_ν is the usual Bessel function.

This expression is well-defined only if it is 2π -periodic with respect to θ . This implies that $m - n/2$ must be an integer. If one enforces this condition and writes $m = n/2 - l$, with l an integer, the expression between the brackets in Eq. (53) is nothing but the sum of two normal modes with the following frequency, azimuthal and axial wave numbers: $(l - n/2 + l\Omega, l, k_z)$ and $(l - n/2 + (l-n)\Omega, l-n, k_z)$. These two modes have also by construction the same radial wave number. They are possible perturbations of the underlying Rankine vortex if they are so-called Kelvin modes, that is if their characteristics satisfy the dispersion relation of the Rankine vortex. To study that condition, it is more convenient to express the frequency of the Kelvin modes in terms of k_r, k_z and l and to write the dispersion relation of the Kelvin modes as $D(l, k_z, \cos \xi) = 0$ with $\cos \xi = k_z / (k_r^2 + k_z^2)^{1/2}$. The condition that the bracket in Eq. (53) is the sum of two Kelvin modes thus reduces at leading order to

$$D(l, k_z, \cos \xi) = D(l-n, k_z, \cos \xi) = 0, \tag{54}$$

with

$$\cos \xi \sim \frac{n}{4|1 + \Omega|}. \tag{55}$$

For a given l , two relations must be simultaneously satisfied for a single parameter k_z . This condition is reminiscent of the condition of resonance of Kelvin modes in the global stability analysis.^{9,10,26} Indeed, Eloy and Le Dizès²⁶ showed for the generalized Moore–Saffman vortex (see also Moore and Saffman¹⁰ for the elliptic case) that the simple resonance of two Kelvin modes with azimuthal wave numbers l and $l - n$ always implies instability. In their analysis, the frequency of the modes, or similarly $\cos \xi$ was not close to a particular value and they computed the growth rate associated with all possible resonance. Here, we focus on the most unstable configurations, which explains why there is the additional condition Eq. (55).

It is important to point out that the local growth rate σ appearing in Eq. (53) varies with respect to the radial coordinate via the local strain rate $s = (n - 1)pr^{n-2}$. For $n \geq 3$, σ^{\max} is then dependent on the radial coordinate: It monotonically increases from the center where it vanishes to the vortex core boundary where it is the largest. Consequently, the radial structure of the perturbation is also dependent on time and evolves such that it becomes localized near the vortex edge for large time. For $n \geq 3$, expression (53) is therefore **not** the expression of two resonant Kelvin modes contrary to what is assumed in the global stability analysis.²⁶ This difference makes the comparison between both analyses difficult. In fact, a comparison is possible only if k_z and l are large. Indeed, in that case, the time-dependence of the radial structure disappears as the perturbation is initially already localized near the vortex edge. The maximum growth rate obtained from Eq. (53) is thus the maximum local growth rate of the vortex edge which is exactly the result obtained by Eloy and Le Dizès²⁶ for the Moore–Saffman vortex when k_z and l go to infinity.

The time-dependence of the radial structure also disappears when $n = 2$ because the growth rate σ is then independent of r . For $n = 2$, expression (53) therefore represents a globally amplified perturbation of the vortex core. The validity of such an expression is based on condition (54) which can be analyzed by plotting the dispersion relation in the $(k_z, \cos \xi)$ plane for two distinct values l and $l + 2$ of the azimuthal wave number. Figures 5(a) and 5(b) display the different branches for $l = \pm 1$ and $l = 0, 2$ respectively. A symmetry of the dispersion relation guarantees that the branches for $l = 1$ collapse with the branches for $l = -1$. For the azimuthal wave number couple $(-1, 1)$, any wave number such that $\cos \xi = 1/(2|1 + \Omega|)$ for one family of branch is then a possible wave number in expression (53). In Fig. 5(a) are circled the possible states for Kirchhoff vortex ($\Omega = 1, \cos \xi_0 = 1/4$) and the Moore–Saffman vortex ($\Omega = 0, \cos \xi_0 = 1/2$). For all the other couples of azimuthal wave number the branches do not collapse. However, as it is seen on Fig. 5(b) for the couple $(0, 2)$, some branches are very close such that one may consider that there is a quasi-resonance. Again, these possible states are indicated by circles for the Kirchhoff vortex and Moore–Saffman vortex at $\cos \xi = 1/4$ and $\cos \xi = 1/2$, respectively. Near resonant states or quasi-resonant states, one expects the growth rate to be given by formula Eq. (32). Its expression in terms of k_z is obtained from the dispersion relation which gives $\cos \xi$ for

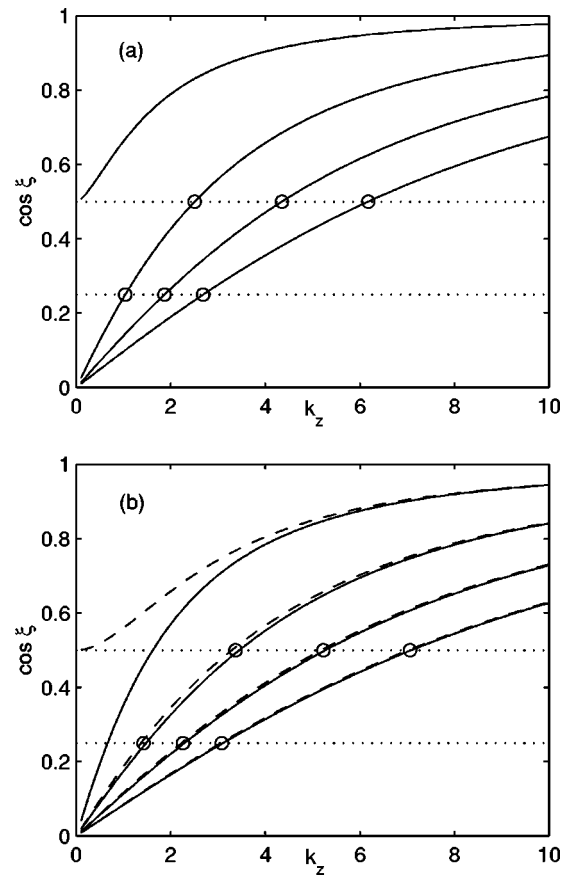


FIG. 5. Dispersion relation of the Rankine vortex in the $(k_z, \cos \xi)$ plane. (a) Modes of azimuthal wave number $m = 1$. (b) Modes of azimuthal wave numbers $m = 0$ (solid lines) and $m = 2$ (dashed lines). Resonant states for the Moore–Saffman vortex and Kirchhoff vortex are indicated by circles at $\cos \xi = 1/2$ and $\cos \xi = 1/4$, respectively.

each k_z . In Figs. 6(a) and 6(b) is shown the growth rate as a function of k_z obtained by this procedure for the Moore–Saffman vortex and Kirchhoff vortex. Both the growth rate associated with perfect resonant modes $(-1, 1)$ and quasi-resonant modes $(0, 2)$ have been plotted.

The destabilization of Kirchhoff vortex by the resonant modes $(-1, 1)$ has been comprehensively analyzed by Miyazaki *et al.*³⁰ They, in particular, compared their numerical results with local stability predictions and with global stability results obtained by Vladimirov and Il'in²⁹ for aspect ratios close to 1. They confirmed the good agreement between the three approaches in predicting the maximum growth rate. Here, we go one step further by providing an estimate for the size of the instability bands using only the local stability result and the dispersion relation of the Kelvin modes. The instability band in terms of $\cos \xi$ is given by expression (35) which reduces to

$$|\cos \xi - \frac{1}{2}| < \frac{9}{32} p \quad \text{for the Moore–Saffman vortex,} \tag{56a}$$

$$|\cos \xi - \frac{1}{4}| < \frac{25}{256} p \quad \text{for the Kirchhoff vortex.} \tag{56b}$$

Using the (dispersion) relation between $\cos \xi$ and k_z , this yields an instability interval of the form

$$|k_z - k_z^{\max}| < \delta k(k_z^{\max}) k_z^{\max} p, \tag{57}$$

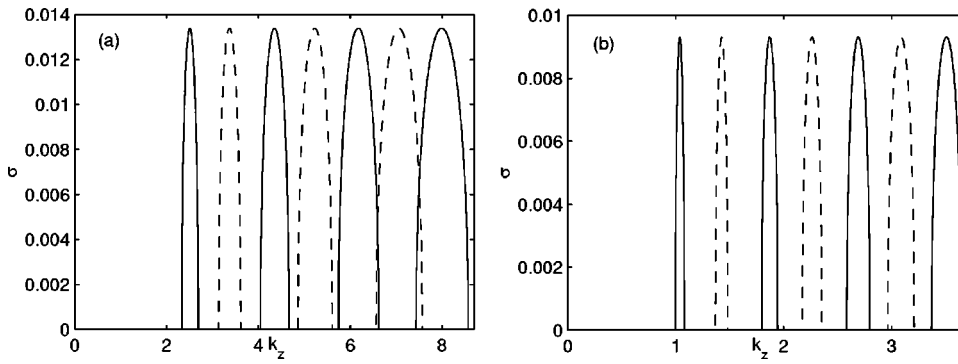


FIG. 6. Growth rate σ versus the axial wave number k_z of the perturbation for a vortex of aspect ratio equal to 1.1. σ and k_z are nondimensionalized with the relative vorticity and the mean radius, respectively. Solid line: Kelvin modes $l = \pm 1$; dashed line: Kelvin modes $l = 0$ and $l = 2$. (a) Moore–Saffman vortex. (b) Kirchhoff vortex.

where k_z^{\max} is a resonant or quasi-resonant wave number (associated with a circle in Fig. 5), and $\delta k(k_z^{\max})$ a function slightly dependent on k_z^{\max} for a given vortex. If one neglects the variation of the radial wave number, i.e., assumes $k_z \tan(\xi)$ as constant near each resonant point, δk is also constant:

$$\delta k = 3/4 \quad \text{for the Moore–Saffman vortex,} \quad (58a)$$

$$\delta k = 5/12 \quad \text{for the Kirchhoff vortex.} \quad (58b)$$

It can be checked on Fig. 7 that this assumption is approximately justified. The results are displayed in Fig. 7(a) for Kirchhoff vortex and Fig. 7(b) for Moore and Saffman vortex. The agreement between the local prediction and the global stability analysis is astonishing. Note, in particular, that for the Moore–Saffman vortex the gap between the simplest local prediction (which neglects the variation of the radial wave number) and the global results is almost entirely filled if one takes into account the variation of the radial wave number.

In Figs. 6(a) and 6(b) have been drawn the instability curves associated with the quasi-resonance (0,2). Surprisingly, this type of resonance has never been analyzed by global or numerical methods for Kirchhoff vortex. For the Moore–Saffman vortex, the global stability analysis has been carried out only recently in Eloy and Le Dizès.²⁶ Their results show that this type of resonance as well as resonance of higher order modes such as (1,3) and so on, can lead to instability with a maximum growth rate comparable to the local maximum growth rate computed here. In all these cases, the local analysis provides a good estimate for the frequency and the instability band width. By contrast, the local analysis developed here, which focuses on the most

unstable configuration, is unable to estimate the characteristics of less unstable configurations. In particular, for the resonance (0,2), Eloy and Le Dizès obtained an unstable mode at $k_z \approx 1.24$ and $\omega \approx 0.83$ with a growth rate only 5% smaller than σ^{\max} . For this value of k_z , the two Kelvin modes $m = 0$ and $m = 2$ satisfy $\cos \xi \approx 0.42$ and $\cos \xi \approx 0.58$, respectively. In terms of inertial waves, this unstable configuration thus corresponds to an interaction of two different waves which differs from the self-interaction process considered in Sec. III. The possibility of resonance of two distinct inertial waves has never been explored in the elliptical instability literature. It would be interesting to extend the analysis to this more general case in order to check whether all the unstable global modes can be correctly recovered from the local analysis.

Quasi-resonance of modes $(m, m + 2)$ are also predicted by the simple self-interaction local analysis. By construction they share the following properties: they have all the same maximum growth rate; the instability bands of all the resonant modes of even azimuthal wave numbers are close to each other and superimpose for large wave numbers; they are separated by the instability bands of resonant modes of odd azimuthal wave numbers which also tend to collapse for large wave numbers. The above estimates Eqs. (58a) and (58b) for the width of the instability band also apply for all the quasi-resonant modes. As a consequence, the instability bands overlap for large wave numbers. These predictions are in agreement with the results obtained by global analysis for the Moore–Saffman vortex.²⁶

Note, finally, that the viscous damping of the global perturbation Eq. (53) is also given by Eq. (45) as all the inertial waves summed to obtain Eq. (53) have the same wave vector

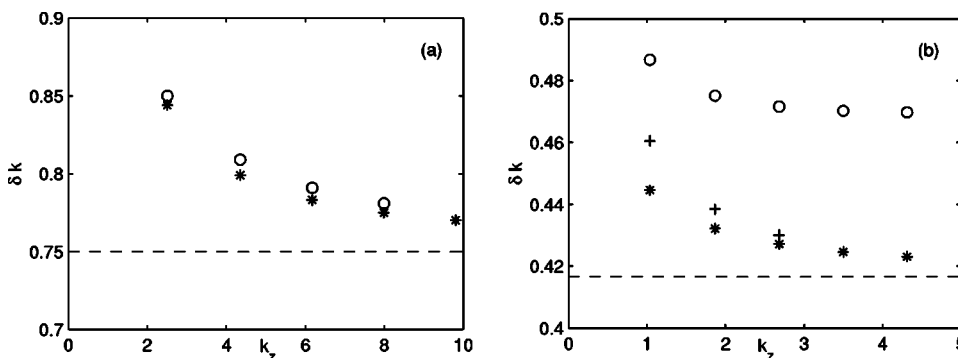


FIG. 7. Instability band width δk versus the axial wave number of the resonant modes $(-1, 1)$. Stars (*): Local stability analysis. Circles (O): global stability analysis. (a) Moore–Saffman vortex. The circles are from Tsai and Widnall (Ref. 9) and Arendt and Fritts (Ref. 31). Dashed line: expression (58a). (b) Kirchhoff vortex. The circles are from Vladimirov and Il'in (Ref. 29). The crosses are deduced from Miyazaki *et al.* (Ref. 30) for an aspect ratio equal to 1.1. Dashed line: expression (58b).

modulus. For the most unstable perturbations, this local estimate is comparable to the one obtained by global analysis.²⁶

B. Stuart vortices in a rotating frame

Stuart vortices are described by the stream function

$$\Psi = \log(\cosh x - \rho \cos y), \tag{59}$$

where ρ is a real parameter between 0 and 1. For $\rho=0$, Eq. (59) reduces to a pure shear-flow with an hyperbolic tangent profile. When $\rho \rightarrow 1$, the solution becomes singular and tends to an array of point vortices of infinite vorticity (but finite circulation). In the intermediate range $0 < \rho < 1$, the solution represents an array of co-rotating vortices with a smooth profile of vorticity. Each vortex is in that case elliptical near its center with a vorticity and a strain rate given in the center by $W_r = (1 + \rho)/(1 - \rho)$ and $s_0 = 1/2$, respectively. The eccentricity of the streamline near the center goes to zero as ρ goes to 1. For ρ close to 1, the maximum growth rate (normalized by W_r) of Stuart vortices in a frame rotating at the angular frequency Ω is therefore given by Eq. (42) with $n=2$ and $p = 2s_0/W_r = (1 - \rho)/(1 + \rho)$.

The global stability properties of Stuart vortices in a rotating frame were recently analyzed in Leblanc and Cambon²⁰ and Potylitsin and Peltier³² (hereafter, referred to as LC98 and PP99). PP99 considered several values of ρ ($\rho = 0.33, 0.5, 0.75$) but a fixed axial wave number $k_z = 2$ for the perturbation, while LC98 only studied the case $\rho = 0.33$ but considered several axial wave numbers. In both studies, Ω was varied between -0.5 and 0.1 (with our definition). For each case, they were able to obtain an unstable branch associated with the elliptical instability of the core. Our goal is here to compare their computed growth rate as Ω varies with the prediction of the local asymptotic theory.

As seen in Sec. IV A, the finite size of the vortex discretizes the possible wave numbers of the perturbations. Moreover, sufficiently close to the vortex center, these perturbations are always combinations of inertial waves. For a fixed axial wave number, one then expects the wave vector angle ξ of the inertial waves to be also discretized. If the instability is due to the inertial wave resonance mechanism explained in Sec. III, the instability growth rate should still be given by Eq. (32). But here, by contrast with the Rankine vortex, no dispersion relation that provides the angle ξ for a given wave number is available. For a given axial wave number, the angle ξ is fixed but cannot be determined from our calculation alone. The local stability theory however predicts that the instability should be maximized when the rotation rate Ω reaches the particular value Ω_{\max} that satisfies Eq. (37). If one replaces $\cos \xi$ by its expression in terms of Ω_{\max} , expression (39) thus provides the following estimate for the growth rate as Ω varies

$$\sigma = \frac{\sqrt{(3 + 2\Omega_{\max})^4 p^2 - 16^2 (1 + \Omega_{\max})^2 (\Omega - \Omega_{\max})^2}}{16(1 + \Omega_{\max})^2}. \tag{60}$$

The most dangerous rotation rate Ω_{\max} obtained by LC98 and PP99 are given in the following table:

	Ω_{\max}	p
$k_z = 10; \rho = 0.33$ (from LC 98)	-0.46	0.5
$k_z = 2; \rho = 0.33$ (from PP 99)	-0.31	0.5
$k_z = 2; \rho = 0.5$ (from PP 99)	-0.24	0.32
$k_z = 2; \rho = 0.75$ (from PP 99)	-0.18	0.14

These values are used to draw the curves displayed in Fig. 8. In these plots are also displayed values taken from the curves of Potylitsin and Peltier³² and Leblanc and Cambon.²⁰

When $\rho = 0.33$, Figs. 8(a) and (b) demonstrate that the asymptotic analysis provides very good estimates for both the maximum value of the growth rate and the width of the unstable region. For larger values of ρ , the growth rate is however slightly overestimated. At first view, this is surprising because the asymptotic theory should *a priori* work better as the vortices become less elliptical. But, in fact, as $\rho \rightarrow 1$, vorticity gradients increase as well, which implies that the local stability properties in the vortex core change more rapidly with respect to the radial coordinate. As a global growth rate is more or less a local growth rate averaged on a fixed area, if the local growth rate decreases more rapidly, the gap between the average and the maximum increases, and this could explain the discrepancy.

LC98 analyzed the stability properties for large axial wave numbers. They showed that the global growth rate is well-estimated by the local growth rate of pure axial waves ($\xi = 0$) at either elliptic or hyperbolic stagnation points. Concerning the elliptic stagnation points, their analysis can be considered as a particular case of the present study. In particular, it can be checked that formula Eq. (44) with $n=2$ reduces to their expression of the local growth rate. Moreover, the good agreement can be explained by the above argument. Indeed, based on what we observed for Rankine vortex, we expect the radial wave number of the perturbation modes to be more or less a constant as k_z varies. It follows that when k_z increases, the angle ξ of the wave vector with respect to the k_z axis goes to zero, and therefore the unstable global modes are only composed of purely axial waves. As shown by LC98, for $k_z = 100$, the pure axial wave prediction is very good. But for $k_z = 10$, Fig. 8(a) shows that it already overestimates the growth rate and our prediction which takes into account the inclination of the wave vector is better.

V. CONCLUSION

This article has focused on the local stability properties of the core of a nonaxisymmetric vortex in a rotating frame. We have shown that an n -fold symmetrical vortex is locally unstable, with a growth rate proportional to the local strain rate s , as soon as the angular frequency Ω of the rotating frame satisfies $|W_a| = |W_r + 2\Omega| > n|W_r|/4$, where W_a and W_r are the absolute and relative vorticities, respectively. The asymptotic analysis has also proved that the instability domain slightly extends below (above) $W_a = nW_r/4$ up to the value $W_a = nW_r/4 - sW_r/2$ if $W_r > 0$ (if $W_r < 0$). An explicit formula [expression (32)] for the leading order growth rate has been obtained as a function of n , Ω and the wave vector angle ξ of the perturbation.

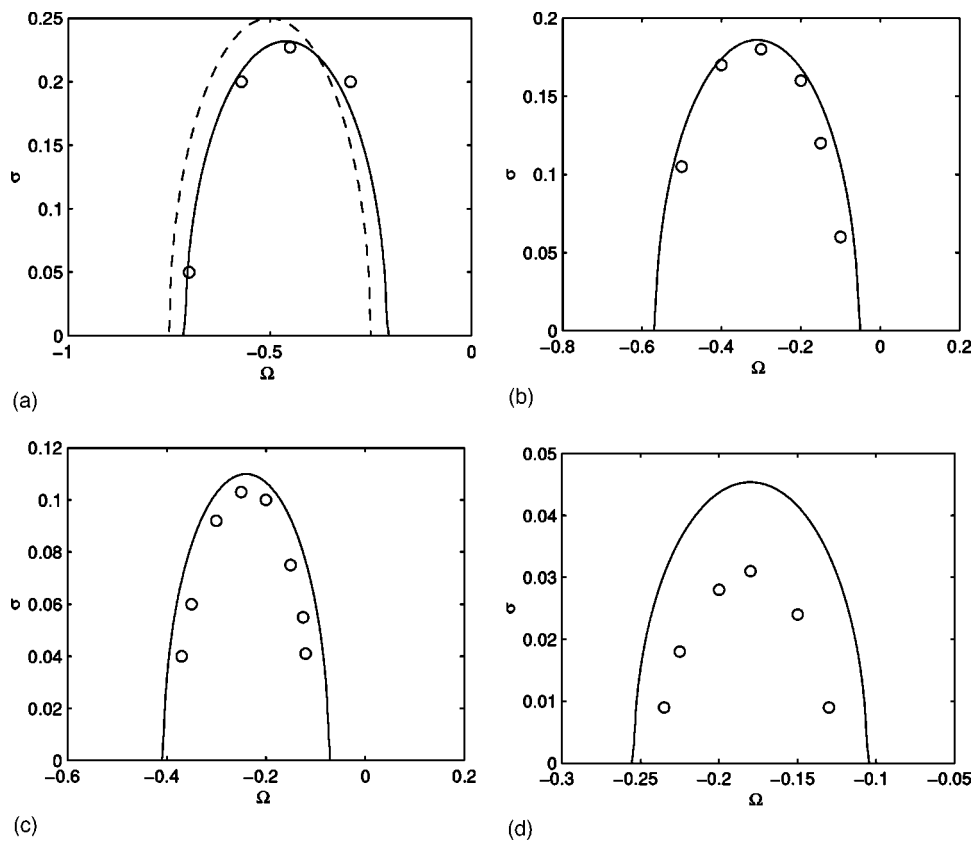


FIG. 8. Maximum growth rate versus the angular frequency Ω of the rotating frame for the perturbations with a fixed axial wave number k_z . The circles are numerical data taken from LC98 (Ref. 20) (a) and PP99 (Ref. 32) (b–d). As explained in the text, the solid curve is the local asymptotic prediction where the angular frequency that gives the maximum value has been taken from the numerical data. (a) $\rho=0.33, k_z=10$; the dashed line is the short-wavelength prediction with pure axial wave vectors ($\xi=0$) given by LC98; (b) $\rho=0.33, k_z=2$; (c) $\rho=0.5, k_z=2$; (d) $\rho=0.75, k_z=2$.

The results have been applied to perturbed Rankine vortices such as the Kirchhoff and Moore–Saffman vortices with an aspect ratio close to 1. From the expression of the most unstable local perturbations, we have shown how global perturbations of the core can be constructed for these vortices. For the elliptic case ($n=2$), these global perturbations have been found to correspond to pairs of resonant normal Kelvin modes of Rankine vortex of azimuthal wave numbers m and $m+2$ in agreement with global stability analysis. However, contrary to the global analysis, the frequency of the most unstable global perturbations is here provided by the calculation. Using the dispersion relation of the Kelvin modes of Rankine vortex, the growth rate of the instability has been obtained as a function of the axial wave number for the Kirchhoff and Moore–Saffman vortices and compared to available results in the literature. The instability bands associated with a resonance of Kelvin modes of azimuthal wave numbers $m=1$ and $m=-1$ has been recovered with a remarkable precision. Other instability bands associated with a resonance $m=0$ and $m=2$ have also been calculated. For the Moore–Saffman vortex, the results have been compared with global stability results and a good agreement has been found for the most unstable modes. For Kirchhoff, the new instability bands associated with this resonance have never been documented elsewhere.

It has also been argued that the local stability analysis could be generalized in order to describe less unstable modes. Contrary to the modes analyzed in this paper which correspond to a self-interaction of a single inertial wave, these other modes would be associated with the interaction of two distinct inertial waves.

The local results have also been applied to the more realistic Stuart vortex. We have shown how both the maximum value of the growth rate and the size of the instability band can be obtained as soon as the most unstable rotation rate is known. A good agreement with numerical data from Leblanc and Cambon²⁰ and Potylytsin and Peltier³² has been demonstrated for Stuart vortices which are not too elliptical nor too concentrated ($\rho=0.33$).

Finally, it is important to again point out that the local stability results are not limited to a specific vortex. For $n=2$, the local analysis is expected to provide good estimates for vortices of aspect ratio up to 2 if the local stability properties do not vary too much on the characteristic radial perturbation wavelength. For these cases, the only information needed from the vortex is the most unstable wave numbers for a given angular rotation or the most dangerous rotation rate for a given wave number. From this information, a complete instability diagram is given by formula Eq. (32) if one neglects the small variation of the radial wave number, which has been found to be justified in the above examples.

For $n>3$, the local instability characteristics vary with the vortex radial coordinate in a similar way as the local strain rate. This nonhomogeneous character makes the local predictions less successful than for $n=2$. Nevertheless, the local analysis still provides the regions where the unstable character is the strongest and the value of the largest possible growth rate. Moreover, analysis of the generalized Moore–Saffman vortex suggests that the growth rate of a global perturbation could be related to a certain average of the local growth rates over the region where the perturbation sits.

ACKNOWLEDGMENTS

This work has benefitted from discussions with Maurice Rossi and Christophe Eloy. They are both warmly acknowledged. I am also grateful to Stéphane Leblanc for having pointed out an inconsistency in the first version of the manuscript.

- ¹E. J. Hopfinger and G. J. F. van Heijst, "Vortices in rotating fluids," *Annu. Rev. Fluid Mech.* **25**, 241 (1993).
- ²B. J. Bayly, "Three-dimensional centrifugal-type instabilities in inviscid two-dimensional flows," *Phys. Fluids* **31**, 56 (1988).
- ³R. C. Kloosterziel and G. J. F. van Heijst, "An experimental study of unstable barotropic vortices in a rotating frame," *J. Fluid Mech.* **223**, 1 (1991).
- ⁴D. Sipp and L. Jacquin, "Three-dimensional centrifugal-type instabilities of two-dimensional flows in rotating systems," *Phys. Fluids* **12**, 1740 (2000).
- ⁵R. T. Pierrehumbert, "Universal short-wave instability of two-dimensional eddies in an inviscid fluid," *Phys. Rev. Lett.* **57**, 2157 (1986).
- ⁶B. J. Bayly, "Three-dimensional instability of elliptical flow," *Phys. Rev. Lett.* **57**, 2160 (1986).
- ⁷F. Waleffe, "On the three-dimensional instability of strained vortices," *Phys. Fluids A* **2**, 76 (1990).
- ⁸S. A. Orszag and A. T. Patera, "Secondary instability of wall-bounded shear flows," *J. Fluid Mech.* **128**, 347 (1983).
- ⁹C.-Y. Tsai and S. E. Widnall, "The stability of short waves on a straight vortex filament in a weak externally imposed strain field," *J. Fluid Mech.* **73**, 721 (1976).
- ¹⁰D. W. Moore and P. G. Saffman, "The instability of a straight vortex filament in a strain field," *Proc. R. Soc. London, Ser. A* **346**, 413 (1975).
- ¹¹A. Lifschitz and E. Hameiri, "Local stability conditions in fluid dynamics," *Phys. Fluids A* **3**, 2644 (1991).
- ¹²T. Miyazaki and Y. Fukumoto, "Three-dimensional instability of strained vortices in stably stratified fluid," *Phys. Fluids A* **4**, 2515 (1992).
- ¹³A. D. D. Craik, "The stability of unbounded two- and three-dimensional flows subject to body forces: Some exact solutions," *J. Fluid Mech.* **198**, 275 (1989).
- ¹⁴C. Cambon, J.-P. Benoit, L. Shao, and L. Jacquin, "Stability analysis and large-eddy simulation of rotating turbulence with organized eddies," *J. Fluid Mech.* **278**, 175 (1994).
- ¹⁵S. Leblanc, "Stability of stagnation points in rotating flows," *Phys. Fluids* **9**, 3566 (1997).
- ¹⁶S. Le Dizès, M. Rossi, and H. K. Moffatt, "On the three-dimensional instability of elliptical vortex subjected to stretching," *Phys. Fluids* **8**, 2084 (1996).
- ¹⁷N. Lebovitz and A. Lifschitz, "Short wavelength instabilities of rotating, compressible fluid masses," *Proc. R. Soc. London, Ser. A* **438**, 265 (1992).
- ¹⁸A. Lifschitz and E. Hameiri, "Localized instabilities of vortex rings with swirl," *Commun. Pure Appl. Math.* **46**, 1379 (1993).
- ¹⁹A. Lifschitz, "On the instability of certain motions of an ideal incompressible fluid," *Adv. Appl. Math.* **15**, 404 (1994).
- ²⁰S. Leblanc and C. Cambon, "Effects of the Coriolis force on the stability of Stuart vortices," *J. Fluid Mech.* **356**, 353 (1998).
- ²¹D. Sipp and L. Jacquin, "Elliptic instability in 2-D flattened Taylor-Green vortices," *Phys. Fluids* **10**, 839 (1998).
- ²²G. K. Forster and A. D. D. Craik, "The stability of three-dimensional time-periodic flows with ellipsoidal stream surfaces," *J. Fluid Mech.* **324**, 379 (1996).
- ²³B. J. Bayly, D. D. Holm, and A. Lifschitz, "Three-dimensional stability of elliptical vortex columns in external strain flows," *Philos. Trans. R. Soc. London, Ser. A* **354**, 895 (1996).
- ²⁴B. Fabijonas, D. D. Holm, and A. Lifschitz, "Secondary instabilities of flows with elliptical streamlines," *Phys. Rev. Lett.* **78**, 1900 (1997).
- ²⁵S. Le Dizès and C. Eloy, "Three-dimensional stability of multipolar vortices," *Phys. Fluids* **11**, 500 (1999).
- ²⁶C. Eloy and S. S. Le Dizès, "Stability of a Rankine vortex in a multipolar strain field," *Phys. Fluids* (submitted).
- ²⁷C. Eloy, Ph. D. thesis, Université Aix-Marseille II, 2000.
- ²⁸C. Eloy, P. Le Gal, and S. Le Dizès, "Experimental study of the multipolar vortex instability," *Phys. Rev. Lett.* (submitted).
- ²⁹V. A. Vladimirov and K. Il'in, "Three-dimensional instability of an elliptical Kirchhoff vortex," *Fluid Dyn.* **3**, 356 (1988).
- ³⁰T. Miyazaki, T. Imai, and Y. Fukumoto, "Three-dimensional instability of Kirchhoff's elliptic vortex," *Phys. Fluids* **7**, 195 (1995).
- ³¹S. Arendt and D. C. Fritts, "The instability of a vortex tube in a weak external shear and strain," *Phys. Fluids* **10**, 530 (1998).
- ³²P. G. Potylytsin and W. R. Peltier, "Three-dimensional destabilisation of Stuart vortices: The influence of rotation and ellipticity," *J. Fluid Mech.* **387**, 205 (1999).
- ³³M. J. Landman and P. G. Saffman, "The three-dimensional instability of strained vortices in a viscous fluid," *Phys. Fluids* **30**, 2339 (1987).
- ³⁴J. Kevorkian and J. D. Cole, *Multiple Scale and Singular Perturbation Methods*, Vol. 114 of *Applied Mathematical Sciences* (Springer, New York, 1996).
- ³⁵H. P. Greenspan, *The Theory of Rotating Fluids* (Cambridge University Press, Cambridge, 1968).
- ³⁶P. Huerre and M. Rossi, in *Hydrodynamics and Nonlinear Instabilities*, edited by C. Godrèche and P. Manneville (Cambridge University Press, Cambridge, 1998), Chap. "Hydrodynamic instabilities in open flows."
- ³⁷D. Sipp, E. Lauga, and L. Jacquin, "Vortices in rotating systems: Centrifugal, elliptic and hyperbolic type instabilities," *Phys. Fluids* **11**, 3716 (1999).
- ³⁸A. D. D. Craik and W. O. Criminale, "Evolution of wavelike disturbances in shear flows: A class of exact solutions of the Navier-Stokes equations," *Proc. R. Soc. London, Ser. A* **406**, 13 (1986).
- ³⁹P. G. Saffman, *Vortex Dynamics* (Cambridge University Press, Cambridge, 1992).
- ⁴⁰G. S. Deem and N. J. Zabusky, "Vortex waves: Stationary 'V states,' interactions, recurrence and breaking," *Phys. Rev. Lett.* **40**, 859 (1978).
- ⁴¹D. W. Moore and P. G. Saffman, "Structure of a line vortex in an imposed strain," in *Aircraft Wake Turbulence*, edited by R. Olsen and Golburg (Plenum, New York, 1971), pp. 339.
- ⁴²S. Kida, "Motion of an elliptic vortex in a uniform shear flow," *J. Phys. Soc. Jpn.* **50**, 3517 (1981).